Research Article

Mona S. Alwhibi, Dina A. Soliman*, Manal A. Awad, Asma B. Alangery, Horiah Al Dehaish, and Yasmeen A. Alwasel

Green synthesis of silver nanoparticles: Characterization and its potential biomedical applications

https://doi.org/10.1515/gps-2021-0039
received May 10, 2021; accepted June 01, 2021

Abstract: In recent times, research on the synthesis of noble metal nanoparticles (NPs) has developed rapidly and attracted considerable attention. The use of plant extracts is the preferred mode for the biological synthesis of NPs due to the presence of biologically active constituents. *Aloe vera* is a plant endowed with therapeutic benefits especially in skincare due to its unique curative properties. The present study focused on an environmental friendly and rapid method of phytosynthesis of silver nanoparticles (Ag-NPs) using *A. vera* gel extract as a reductant. The synthesized Ag-NPs were characterized by transmission electron microscopy (TEM), UV-Vis spectroscopy, Fourier transform infrared (FTIR), and dynamic light scattering (DLS). TEM micrographs showed spherical-shaped synthesized Ag-NPs with a diameter of 50–100 nm. The UV-Vis spectrum displayed a broad absorption peak of surface plasmon resonance (SPR) at 450 nm. The mean size and size distribution of the formed Ag-NPs were investigated using the DLS technique. Antibacterial studies revealed zones of inhibition by Ag-NPs of *A. vera* (9 and 7 mm) against *Pseudomonas aeruginosa* and *Escherichia coli*, respectively. Furthermore, the antifungal activity was screened, based on the diameter of the growth inhibition zone using the synthesized Ag-NPs for different fungal strains. Anticancer activity of the synthesized Ag-NPs against the mouse melanoma F10B16 cell line revealed 100% inhibition with Ag-NPs at a concentration of 100 μg mL^{-1}. The phyto-synthesized Ag-NPs demonstrated a marked antimicrobial activity and also exhibited a potent cytotoxic effect against mouse melanoma F10B16 cells. The key findings of this study indicate that synthesized Ag-NPs exhibit profound therapeutic activity and could be potentially ideal alternatives in medicinal applications.

Keywords: *Aloe vera*, phytosynthesis, silver nanoparticle, antitumor, antimicrobial activities

1 Introduction

Nanotechnology includes the synthesis of nanoparticles (NPs) with varied morphology, size, and controlled dispersity to be used for their benefits in several ways. It has the potential to impact human society for being widely used in various fields of science and technology [1].

Antimicrobial, dental therapy, wound healing, surgery function, catalyst, and biomedical devices are just a few applications of metal NPs [2]. Because of their unique optical and electrical properties, NP-based drugs have been found to be more efficacious [3,4]. Surface plasmon resonance (SPR) is a well-known property of NPs that increases their effectiveness [5].

Silver nanoparticles (Ag-NPs) remarkably, have a narrow plasmon resonance, a high surface-to-volume ratio, special physicochemical properties, and a wide range of applications in medical research, microelectronics, and biological activities [6,7]. AgNPs have garnered considerable interest among other metal NPs due to their wide use in several commercial and pharmacologically significant products [8,9]. Considering the synthesis, the traditional methods such as the physical, thermal, hydrothermal, and chemical synthesis modes are expensive,

* **Corresponding author: Dina A. Soliman,** Department of Botany and Microbiology, College of Science, King Saud University, P.O. Box 22452, Riyadh, 11495, Kingdom of Saudi Arabia, e-mail: dsoliman@ksu.edu.sa
Mona S. Alwhibi, Horiah Al Dehaish, Yasmeen A. Alwasel: Department of Botany and Microbiology, College of Science, King Saud University, P.O. Box 22452, Riyadh, 11495, Kingdom of Saudi Arabia
Manal A. Awad: Department of Physics, College of Science, King Saud University, P.O. Box 22452, Riyadh, 11495, Kingdom of Saudi Arabia
Asma B. Alangery: Department of Chemistry, College of Science, King Saud University, P.O. Box 22452, Riyadh, 11495, Kingdom of Saudi Arabia

extremely hazardous and make use of toxic chemicals. Therefore, the emphasis is on a green synthesis approach making use of biological resources for the efficient formulation of NPs [10–12]. The cornerstone of this sustainable method is the use of renewable materials and environmentally benign compounds as reducing/capping agents to synthesize green nanoparticles [13]. Methods of green synthesis have been effectively utilized to synthesize NPs using different biomolecules, such as vitamins, yeasts, enzymes, algae, biodegradable polymers, and microorganisms, and plant parts such as leaf, stem, gum, fruit, bark, shells, roots, buds, and flowers [12,14].

Aloe vera (*A. vera*) is a succulent plant with thorns in its branches with a waxy coating that grows easily in arid conditions [15,16]. *A. vera* leaves have three layers: the outer layer is a thick and protective layer which has a high proportion of cellulose; the middle layer contains major flavanone (aloin A and B), and the inner layer has a fresh gel that contains an acetylated glucomannan, sugars, vitamins (A, B, C, and E), amino acids, proteins, and anthraquinones [17–19]. *A. vera* gel is utilized in many cosmetic products especially skincare. It is also considered to be effective for treating burns and wounds, which is known for its soothing effect on the affected skin. It can also be used to treat a wide range of health-related disorders [20]. The antimicrobial property and biomedical applications of AgNPs synthesized with *A. vera* gel extract are well investigated. However, very few studies have reported and documented the use of *A. vera* gel to synthesize AgNPs for biomedical applications.

With this premise, the present study aimed at the synthesis of *A. vera* gel extract for phytosynthesis of AgNPs and the investigation of their promising biomedical applications based on the antimicrobial and anticancer activities.

2 Materials and methods

2.1 Identification of plant

Aloe vera was collected from a local park at King Saud University, girls campus, Riyadh, Saudi Arabia, and identified at the Taxonomy Laboratory No. 116, Botany Department, King Saud University, Riyadh.

2.2 Preparation of plant extract

The healthy large outer leaves close to the ground were selected. They were then cut carefully at a slight angle, and the leaves were placed upright in a slightly tilted container for roughly 10 min, allowing much of the sap and the gel to drain out. About 20 g of the collected gel was weighed and transferred into a 500 mL conical flask containing 100 mL of deionized water, mixed well, and heated for 45 min in a water bath. The resulting solution was centrifuged at 5,000 rpm for 15 min, filtered using Whatman number 1 filter paper, and then the filtrate was stored at 4°C for further use.

2.3 Synthesis of Ag-NPs

An aqueous solution of silver nitrate ($AgNO_3$) was prepared using 2 mM $AgNO_3$ powder dissolved in 100 mL of deionized water at a fixed ratio. The reaction mixture was prepared by taking 10 mL of the above-prepared filtrated extract obtained from the plant and 40 mL of the $AgNO_3$ solution, with incubation at 80°C for up to 45 min. The reduction of Ag ions was observed by the change of color from colorless to light yellow and then to dark brown (Figure 1).

2.4 Characterization of synthesized Ag-NPs

The absorption spectrum and SPR of the formed Ag-NPs were recorded using a UV-Vis (PerkinElmer, Waltham, MA, USA). The functional groups in the Ag-NP samples and *A. vera* gel extract were investigated via Fourier transform infrared (FTIR) spectroscopy (Nicolet 6700,

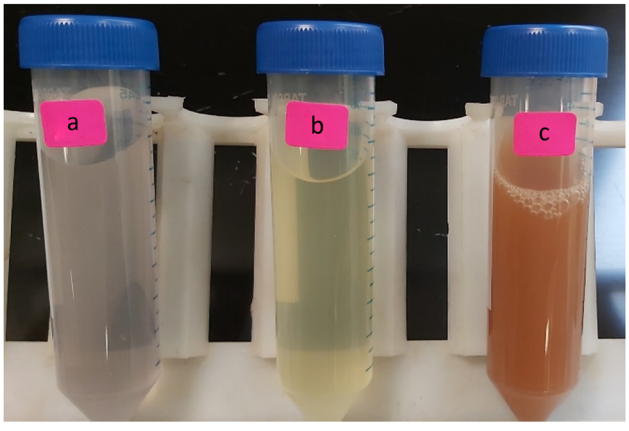

Figure 1: *A. vera* gel extract (a), a mixture of aqueous silver nitrate and gel extract after 10 min (b), and after 45 min (c), production of Ag-NPs using *A. vera* gel extract as green reducing.

Thermo Scientific, USA), using the potassium bromide (KBr) pellet technique. Transmission electron microscopy (TEM) (JEOL-JEM-1011, Japan) was used to examine the size and morphology of the phytosynthesized Ag-NPs with an acceleration voltage of 80 kV. The particle size distribution of the NPs, hydrodynamic diameter, and polydispersity index (PdI) were determined and measured by dynamic light scattering (DLS) particle size analyzer (ZEN3600 Malvern, Nano series, HT Laser, Malvern, UK).

2.5 AgNP biomedical activities

2.5.1 Cytotoxicity of synthesized Ag-NPs

The anti-proliferative activity of the Ag-NPs against mouse melanoma B16F10 cell lines was analyzed by the MTT assay using a 96-well plate supplemented with different concentrations of *A. vera* extract and Ag-NPs. The plates were incubated for 5 h at 37°C. Then, 0.1 mL of 1% trypan blue exclusion test was added. Cells were seeded in a 96-well plate at a density of 1×10^5 cells/well in a 90 µL Dulbecco's modified Eagle's medium. The cells were then allowed to settle before starting treated with different (3.125, 6.25, 12.5, 25, 50, and 100 µg mL^{-1}) concentrations of the samples. The treated cells were allowed to grow further for 24 h. The experiment was performed on four replicates. Specifically, the non-viable cells adopted a blue color while the live cells did not take on the color of the dye. Then, the numbers of blue-stained and unstained cells were determined. The cell viability of the untreated cells was 100% and that of the treated cells was below 100%.

2.5.2 Antibacterial activity

Nutrient agar medium was prepared by dissolving 14 g of agar powder in 500 mL of distilled water and then autoclaved. A total of 20 mL of prepared agar was poured into each Petri dish, which was left to stand for 15 min for the agar to solidify, then the plates were inoculated overnight with human pathogens, such as the Gram-negative strain, *Escherichia coli* ATCC35218, and the gram-positive strains, *Staphylococcus aureus* ATCC 43300, *Enterococcus faecalis* ATCC 29212, and *Bacillus cereus* ATCC 11778 (clinical isolate) obtained from King Khalid University Hospital, Riyadh, Saudi Arabia. All organisms were tested simultaneously by the disc diffusion method [21]. Synthesized Ag-NPs and pure extract of *A. vera* were added steadily until the wells were full, followed by incubation at 37°C for 24 h. The diameter of the zone of inhibition was measured.

2.5.3 Antifungal activity

The samples were assayed for antifungal activity against bipolar heterothallic, *Fusarium oxysporum* and *Macrophomina*. These fungal strains were grown on a potato dextrose agar plate at 28°C. A total of 500 mL of the medium, which was prepared by dissolving 19 g of agar in 500 mL of distilled water, was autoclaved. A volume of 250 µL of synthesized Ag-NPs and pure extract of A. *vera*, separately, were added to a sterile petri dish, followed by pouring of the sterilized medium with gentle mixing. Fungal discs with a diameter of 6 mm, which were grown for 7 days from cultures of the above-mentioned fungi, were placed aseptically in the middle of the plate. The plates were incubated for 7–14 days at 28°C. The antifungal activity was estimated by measuring the diameter of the inhibition zone.

3 Results and discussion

3.1 UV-Vis spectral analysis

The phytosynthesis of Ag-NPs using *A. vera* gel extract as a reducing and stabilizing agent was primarily evidenced by the change in color of the reaction from light yellow to brown (Figure 1). The change in color confirmed the formation of Ag-NPs, due to the excitation of SPR vibration in these particles [22]. The position of the SPR band in UV-Vis spectra is sensitive to particle shape, size, interaction with the medium, local refractive index, and the extent of charge transfer between medium and the particles [23,24]. The UV-Vis spectral analysis identified a broad peak at approximately 450 nm, indicating the phytosynthesis of Ag-NPs (Figure 2). From the UV spectrum, it was observed that the absorption peak was broader, indicating the presence of particles with a wide size distribution. This result is in line with the findings of a previous study [25].

3.2 FTIR analysis

The FTIR absorption spectra of the *A. vera* gel aqueous extract and the formation of Ag-NPs are shown in Figure 3. The top spectrum of Figure 3 presents the FT-IR spectrum

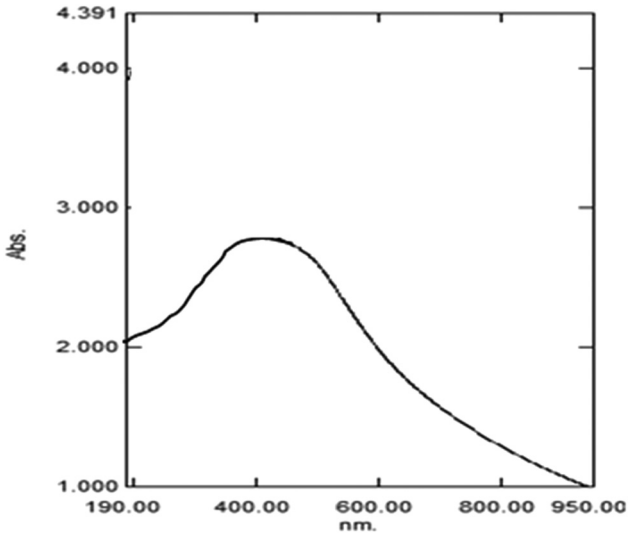

Figure 2: UV-Vis spectra of Ag-NPs produced by *A. vera* extract.

of pure *A. vera* gel extract, showing absorption peaks at 340.733, 1621.13, 1362.92, 1035.99, 777.12, 523.46, and 468.84 cm^{-1}. These absorbance bands were identified to be associated with the stretching vibrations for O–H (hydrogen-bonded alcohols and phenols). The bottom spectrum of Figure 3 shows the FT-IR bands of green Ag-NPs and identifies the possible functional groups in the suspension. The absorpion peaks located at 2931.21, 1731.86, 1428.84, 1248.00, and 1039.00 cm^{-1} were suggested to indicate the presence of an amide group or proteins. These results indicate that the carbonyl group of proteins adsorbed strongly to metals, indicating that proteins could also have formed a layer along with the bio-organics, securing interactions with phytosynthesized NPs; they also show that their secondary structure was not affected during the reaction with Ag ions or after binding with Ag-NPs [26]. In addition, biomolecules in the extract have a strong ability to bind metal, suggesting the formation of a layer covering metal NPs and acting as a capping agent to prevent agglomeration and providing stability in the medium [26,27].

3.3 DLS measurements analysis

DLS is one of the most multifunctional techniques used for identifying the size and size distribution of NPs. The DLS measurements of the average size of Ag-NPs are depicted in Figure 4. The average size of the formed Ag-NPs was about 82 nm, while the PdI value was 0.134. The PdI value represents the monodispersity of the NPs. DLS technique determines the hydrodynamics of nanoparticle size and is measured in an aqueous suspension containing metallic core, ions, and biological biomolecules attached to the surface of NPs [28,29].

3.4 TEM images of Ag-NPs

The size and morphology of the Ag-NPs were examined using TEM. TEM images of the phytosynthesized Ag-NPs are shown in Figure 5. The diameter of the particles was determined to be in the range of 5–10 nm, which was smaller than the result obtained by DLS. TEM images presented monodisperse Ag-NPs with a mostly spherical shape. These results are in agreement with previous

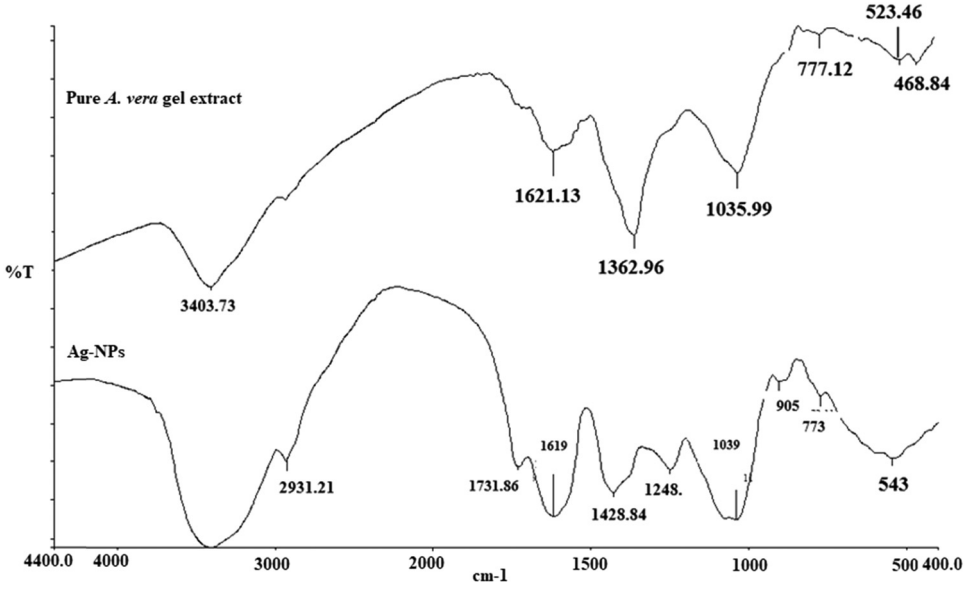

Figure 3: FTIR spectra of pure *A. vera* gel extract and the phytosynthesized Ag-NPs.

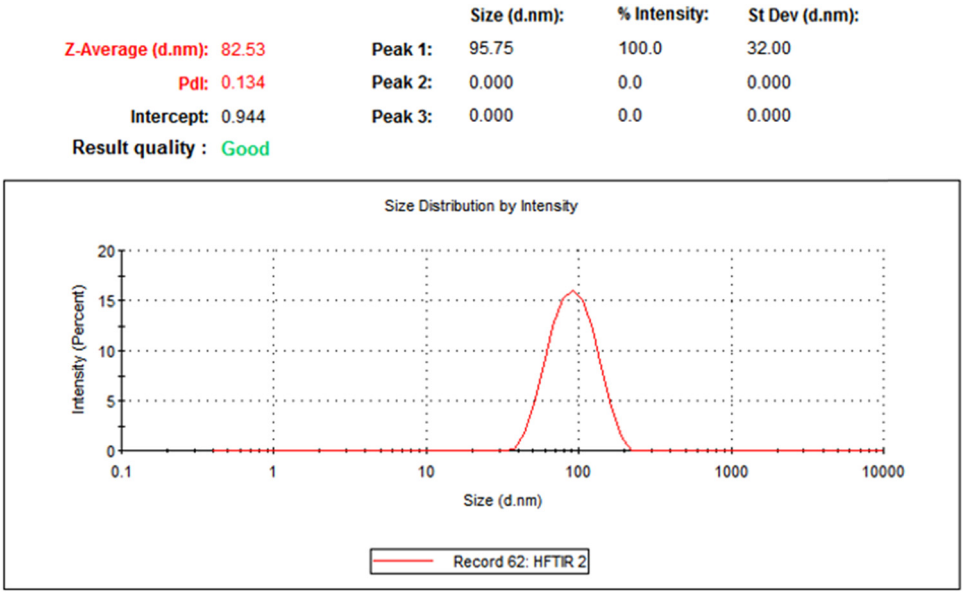

Figure 4: DLS measurement of the average size of phytosynthesized Ag-NPs.

studies by Mohamed et al. and Tippayawat et al. who reported spherical Ag-NPs synthesized using *Aloe vera* extract between 70 and 190 nm in size [30,31].

3.5 Cytotoxic effects

The effect of different concentrations (3.125, 6.25, 12.5, 25, 50, and 100 µg mL^{-1}) of Ag NPs on the *B16F10* cell line has been assessed using an *in-vitro* MTT assay. The results suggested that phytosynthesized Ag-NPs showed marked cytotoxic activity against the *B16F10* cancer cell line. The cytotoxic effect of the synthesized Ag-NPs at the highest concentration (100 µg mL^{-1}) was more profound on *B16F10* cells as compared to the standard anti-cancer drug, NSAID used as a positive control (Figure 6).

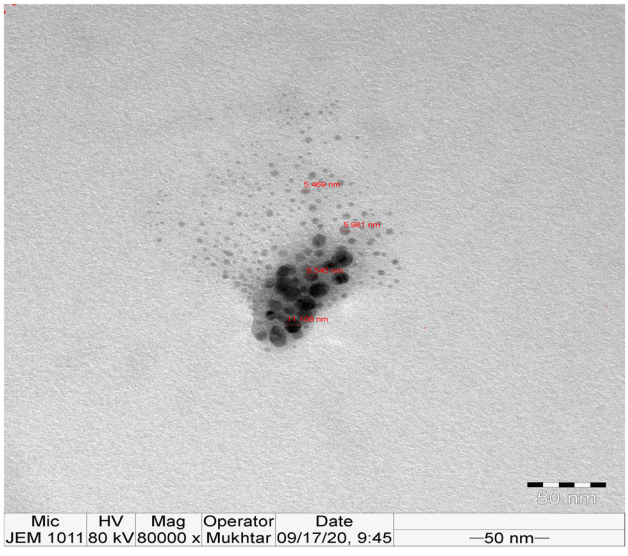

Figure 5: TEM image of phytosynthesized Ag-NPs.

Thus, the cell viability of the cancer cell line decreased with the increasing concentration of synthesized Ag-NPs. At low concentration (3.125 µg mL^{-1}), approximately 100% cell viability was established, while at 50 µg mL^{-1} (IC_{50}), cell viability was 69.94%, and at 100 µg mL^{-1} concentration, the cell viability was reduced to 2.14% against 18.5% with the standard drug (positive control) (Figure 6). To the best of our knowledge, this is the first study that evaluated the cytotoxicity of Ag-NPs synthesized with *A. vera* gel extract on B16F10 cancer cell line. However, the cytotoxic effect of AgNPs synthesized with *A. vera* leaf extract has been previously reported against different cancer cell lines. For instance, Mohamed et al. [30] reported the anti-tumor activity of Ag-NPs against human MCF7 breast cancer cell line and found that at a high concentration of 200 µg mL^{-1}, the cell viability was 28.7%. Tippayawat et al. [31] determined the cytotoxicity of Ag-NPs@ *A. vera* on PBMCs human cells. The % survival of the cells in less than 0.0025 mg mL^{-1} of both NPs was significantly higher than 50%, which confirms that these AgNPs@AVs were non-toxic to human PBMCs and had a promising future in therapeutics.

Many studies have reported that the cytotoxic effect of Ag-NPs could be caused by intracellular oxidative stress, which causes damage to cellular components such as lipids, DNA, and proteins, ultimately leading to

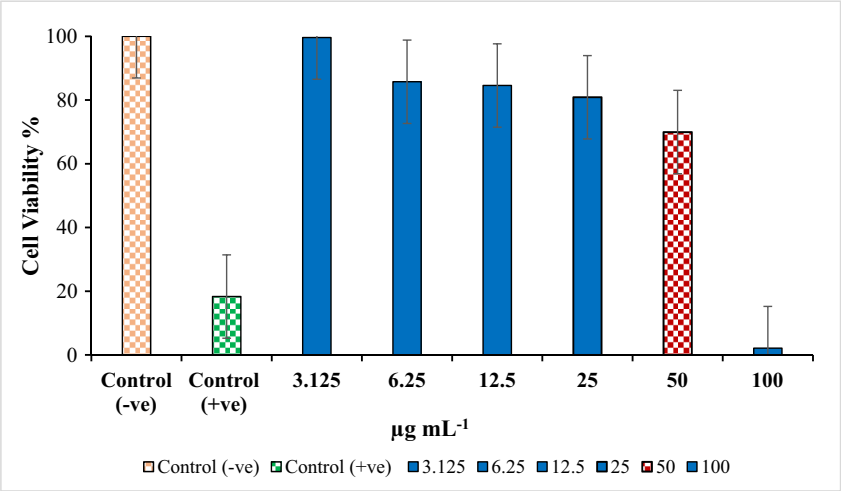

Figure 6: *In vitro* cytotoxic activity of Ag-NPs synthesized using *Aloe vera* gel extract against *B16F10* cell line.

cell death [18,32]. On the other hand, the anticancer activity of Ag-NPs may be due to Ag^+ ions, which suggests that a significant amount of Ag^+ ions will inhibit the sarcoplasmic reticulum which leads to cell death [33].

3.6 Antibacterial activity

The disc-diffusion method has been utilized to screen the antimicrobial activity of green synthesized Ag-NPs against a different strain of microbes: G+ bacteria (*Enterococcus faecalis*, *Staphylococcus aureus*, *Bacillus cereus*) G– bacteria (*Escherichia coli*).

Aloe vera extract did not show any inhibition in the bacterial growth in all the strains of bacteria evaluated. Figure 7 shows the inhibition zones (mm) around the disk containing green synthesized Ag-NPs at different concentrations (5 and 10 µg mL^{-1}). At a higher concentration of 10 µg mL^{-1}, synthesized Ag-NPs were more effective than the lower concentration (5 µg mL^{-1}). The synthesized Ag-NPs showed the maximum zone inhibition (9.1 ± 0.100 mm) against *P. aeruginosa* and followed by *E. coli* (7.0 ± 0.000 mm), *S. aureus* (4.1 ± 0.100 mm), and *B. cereus* (2.03 ± 0.0577 mm)

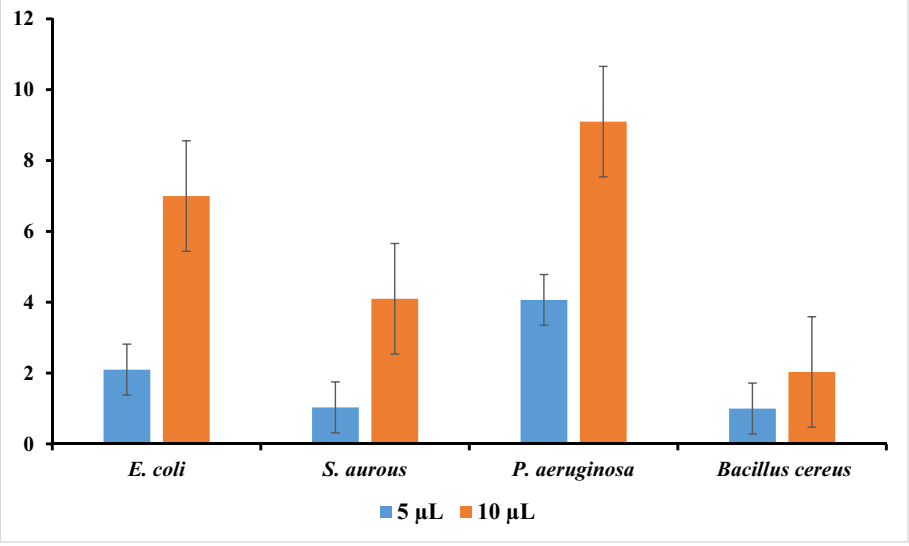

Figure 7: The sizes of inhibition zones (mm) representing antibacterial activity of aqueous extract of *Aloe vera* (blue columns) and the synthesized Ag-NPs of *Aloe vera* (orange columns): *E. coli*, *S. aureus*, *Pseudomonas aeruginosa*, and *B. cereus*. Different letters within a particular concentration show the statistical difference ($p \geq 0.05$).

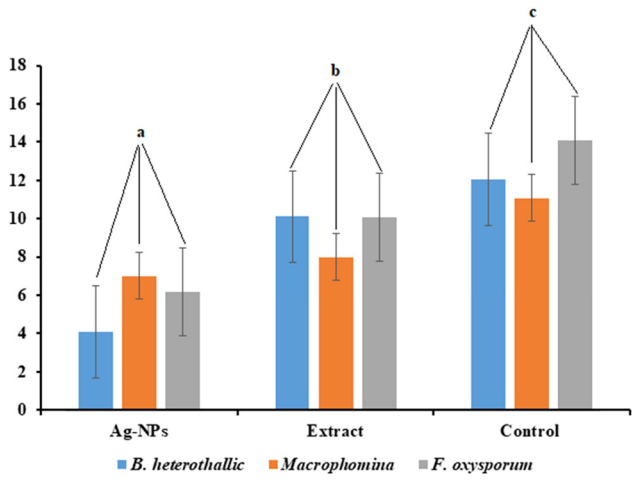

Figure 8: Antifungal activity of pure extract of *A. vera* (a), Ag-NPs produced using *A. vera* (b), and control (c). Different letters show a significant difference ($p \geq 0.05$) between the treatments and control.

at a concentration of 100 μg mL^{-1}. The synthesized Ag-NPs at a concentration of 100 μg mL^{-1} exhibited a significant ($p \geq 0.05$) anti-bacterial effect on *P. aeruginosa* as compared to the other strains. The antibacterial activity of synthesized Ag-NPs increased in a dose-dependent manner. Similar results were reported in a study by Anju and Tippayawat [18,31] which showed that Ag-NPs synthesized using *Aloe vera* leaves extract showed similar antibacterial activity against various bacterial strains.

Various mechanisms have been proposed for the antibacterial activity of Ag-NPs in previous studies [34]. Some studies reported that Ag-NPs exhibited antimicrobial effects against bacterial cells via (a) membrane disruption due to the association/interaction of Ag-NPs with DNA and other biomolecules, subsequently causing inhibition of cell multiplication, and (b) formation of reactive oxygen species through interaction with enzymes and/or biomolecules, leading to cellular damage [35].

Gram-positive bacteria possess a thick cell wall of the peptidoglycan layer composed of linear polysaccharide chains, cross-linked by short peptides, which is a rigid structure that hinders the penetration of AgNPs into the bacterial cell wall, compared to Gram-negative bacteria where the cell wall consists of a thinner peptidoglycan layer [36–38].

The findings of the anti-fungal activity test show that the prepared AgNPs have marked antifungal activity against *Bipolar heterothallic*, *Fusarium oxysporum*, and *Macrophomina* as shown in Figure 8. The maximum fungal growth inhibition by the prepared AgNPs was observed for *B. heterothallic* (4 mm), followed by *F. oxysporum* and *Macrophomina* (6 and 7 mm, respectively). Taken together, for all the fungal strains, the synthesized AgNPs showed a significant ($p \geq 0.05$) anti-fungal activity compared to the *A. vera* extract and control without treatment that exhibited complete fungal growth as shown in Figure 8. This result can be attributed to the lack of any active antimicrobial compounds in the extracellular extract. It has been recognized that there are several factors that contribute to the antimicrobial activity of Ag-NPs, including their shape, size, and surface charge, the tolerance to Ag-NPs, species-sensitivity, the type, genus, and species of the bacteria, the concentration of the NPs, and the duration of exposure to the pathogens [39]. The observed results showed the capability of AgNPs to prevent the fungal growth in the plates.

Whereas the mechanism for AgNPs fungicidal activity is unknown, it has been proposed that AgNPs inhibit the budding process by forming pores on the fungal cell membrane, which can lead to cell death [40]. It has been proposed that AgNP's antibacterial activity is mediated by the formation of free radicals, membrane damage, and the formation of pits on the surface of the bacterial cell wall membrane. Furthermore, the production of free radicals can alter the chemical structure of DNA and proteins [40].

4 Conclusion

The present study is significant in the field of nanotherapeutics in terms of the phytosynthesis of Ag-NPs using *A. vera* gel extract which is an ecofriendly procedure that is relatively inexpensive, rapid, facile, and does not require any toxic chemicals. The synthesized NPs have been characterized using UV-Vis, DLS, FTIR, and TEM. The green synthesized NPs were spherical in shape, with an average size of 82 nm in diameter. Additionally, these NPs exhibited marked antimicrobial activity against different bacterial and fungal strains. Further, the findings also showed the AgNPs' potential cytotoxicity against viable cells from the *B16-F10* melanoma cell line. These findings open up new possibilities to utilize the NPs synthesized from *A. vera* gel extract for a wide range of applications including, pharmaceutical, cosmetic, biomedical, and nanomedical fields.

Acknowledgments: The authors extend their appreciation to the Researchers Support Project (number RSP-2021/173) of King Saud University.

Funding information: The authors extend their appreciation to the Researchers Support Project (number RSP-

2021/173) of King Saud University, Riyadh, Saudi Arabia, for payment of the charge for publishing this manuscript.

Author contributions: Mona S. Alwhibi: funding acquisition, validation, supervision, formal analysis, project administration; Dina A. Soliman: visualization, resources, data curation, formal analysis, methodology, writing – original draft; Manal A. Awad: writing – review and editing, resources, formal analysis; Asma B. Alangery: data curation; Horiah Al Dehaish: resources; Yasmeen A. Alwasel: data curation.

Conflict of interest: The authors declare no competing financial interests.

Reference

[1] Siddiquee MA, Ud din Parray M, Mehdi SH, Alzahrani KA, Alshehri AA, Malik MA, et al. Green synthesis of silver nanoparticles from Delonix regia leaf extracts: in-vitro cytotoxicity and interaction studies with bovine serum albumin. Mater Chem Phys. 2020;242:122493.

[2] Tade RS, Nangare NS, Patil PO. Agro-industrial waste-mediated green synthesis of silver nanoparticles and evaluation of its antibacterial activity. Nano Biomed Eng. 2020;12(1):57–66.

[3] Smith BR, Gambhir SS. Nanomaterials for in vivo imaging. Chem Rev. 2017;117(3):901–86.

[4] Kumar V, Singh S, Srivastava B, Bhadouria R, Singh R. J Environ Chem Eng. 2019;7(3):103094.

[5] Jabir MS, Hussien AA, Sulaiman GM, Yaseen NY, Dewir YH, Alwahibi MS, et al. Green synthesis of silver nanoparticles from Eriobotrya japonica extract: a promising approach against cancer cells proliferation, inflammation, allergic disorders and phagocytosis induction. Artif Cells Nanomed Biotechnol. 2021;49(1):48–60.

[6] Gul AR, Shaheen F, Rafique R, Bal J, Waseem S, Park TJ. Grass-mediated biogenic synthesis of silver nanoparticles and their drug delivery evaluation: a biocompatible anti-cancer therapy. Chem Eng J. 2021;407:127202.

[7] Nouri AF, Yaraki MT, Lajevardi AD, Rezaei ZE, Ghorbanpour MA, Tanzifi M. Ultrasonic-assisted green synthesis of silver nanoparticles using Mentha aquatica leaf extract for enhanced antibacterial properties and catalytic activity. Colloids Interface Sci Commun. 2020;35:100252.

[8] Das G, Shin HS, Kumar A, Vishnuprasad CN, Patra JK. Photo-mediated optimized synthesis of silver nanoparticles using the extracts of outer shell fiber of *Cocos nucifera* L. fruit and detection of its antioxidant, cytotoxicity and antibacterial potential. Saudi J Biol Sci. 2021;28(1):980–7.

[9] Mohammed SS, Lawrance AV, Sampath S, Sunderam V, Madhavan Y. Facile green synthesis of silver nanoparticles from sprouted Zingiberaceae species: spectral characterization and its potential biological applications. Mater Tech. 2021;35:1–4.

[10] Gul AR, Shaheen F, Rafique R, Bal J, Waseem S, Park TJ. Grass-mediated biogenic synthesis of silver nanoparticles and their drug delivery evaluation: a biocompatible anti-cancer therapy. Chem Eng J. 2020;407:127202.

[11] Nasrollahzadeh M, Sajjadi M, Maham M, Sajadi SM, Barzinjy AA. Biosynthesis of the palladium/sodium borosilicate nanocomposite using *Euphorbia milii* extract and evaluation of its catalytic activity in the reduction of chromium(VI), nitro compounds and organic dyes. Mater Res Bull. 2018;102:24–35.

[12] Mahdiani M, Soofivand F, Ansari F, Salavati-Niasari M. Grafting of CuFe12O19 nanoparticles on CNT and graphene: eco-friendly synthesis, characterization and photocatalytic activity. J Clean Prod. 2018;176:1185–97.

[13] Rasli NI, Basri H, Harun Z. Zinc oxide from aloe vera extract: two-level factorial screening of biosynthesis parameters. Heliyon. 2020;6(1):e03156.

[14] Mankodi H. Studies on different type of sutures using aloe vera gel coating. Int J Text Fashion Technol. 2013;4:11–6.

[15] Nandal U, Bhardwaj R. Aloe vera: a valuable wonder plant for food, medicine and cosmetic use – a review. Int J Pharm Sci Rev Res. 2012;1:59–67.

[16] Chow JT, Williamson DA, Yates KM, Goux WJ. Chemical characterization of the immunomodulating polysaccharide of *Aloe vera* L. Carbohydr Res. 2005;340(6):113142.

[17] Reynolds T, Dweck AC. Aloe vera leaf gel: a review update. J Ethnopharmacol. 1999;68:3–37. doi: 10.1016/s0378-8741(99)00085-9.

[18] Anju TR, Parvathy S, Veettil MV, Rosemary J, Ansalna TH, Shahzabanu MM, et al. Green synthesis of silver nanoparticles from *Aloe vera* leaf extract and its antimicrobial activity. Mater Today Proc. 2021 Mar 12;43:3956–60.

[19] Zaidan MR, Noor A, Badrul AR, Adlin A, Norazah A, Zakiah I. In vitro screening of five local medicinal plants for antibacterial activity using disc diffusion method. Trop Biomed. 2005;22(2):165–70.

[20] Noginov MA, Zhu G, Bahoura M, Adegoke J, Small C, Ritzo BA, et al. The effect of gain and absorption on surface plasmons in metal nanoparticles. Appl Phys B. 2007;86:455–60. doi: 10.1007/s00340-006-2401-0.

[21] Vidhu VK, Aromal SA, Philip D. Green synthesis of silver nanoparticles using Macrotyloma uniflorum. Spectrochim Acta A Mol Biomol Spectros. 2011;83(1):392–7.

[22] Boken J, Khurana P, Thatai S, Kumar D, Prasad S. Plasmonic nanoparticles and their analytical applications: a review. Appl Spectrosc Rev. 2017;52(9):774–820.

[23] Rajkumar T, Sapi A, Das G, Debnath T, Ansari A, Patra JK. Biosynthesis of silver nanoparticle using extract of Zea mays (corn flour) and investigation of its cytotoxicity effect and radical scavenging potential. JPPBEG. 2019;193:1–7.

[24] Medda S, Hajra A, Dey U, Bose P, Mondal NK. Biosynthesis of silver nanoparticles from Aloe vera leaf extract and antifungal activity against *Rhizopus* sp. and *Aspergillus* sp. Appl Nanosci. 2015;5(7):875–80.

[25] Awad AM, Salem NM, Abdeen AO. Green synthesis of silver nanoparticles using carob leaf extract and its antibacterial activity. Int J Ind Chem. 2013;4(1):1–6.

[26] Aslany S, Tafvizi F, Naseh V. Characterization and evaluation of cytotoxic and apoptotic effects of green synthesis of silver

nanoparticles using Artemisia Ciniformis on human gastric adenocarcinoma. Mater Today Commun. 2020;24:101011.
[27] Gupta A, Koirala AR, Gupta B, Parajuli N. Improved method for separation of silver nanoparticles synthesized using the Nyctanthes arbor-tristis shrub. ACMY. 2019;3(1):35–42.
[28] Moteriya P, Chanda S. Green synthesis of silver nanoparticles from *Caesalpinia pulcherrima* leaf extract and evaluation of their antimicrobial, cytotoxic and genotoxic potential (3-in-1 system). J Inorg Organomet Polym. 2020;30:3920–32. doi: 10.1007/s10904020-01532-7.
[29] Xia T, Kovochich M, Brant J, Hotze M, Sempf J, Oberley T, et al. Comparison of the abilities of ambient and manufactured nanoparticles to induce cellular toxicity according to an oxidative stress paradigm. Nano Lett. 2006;6(8):1794–807.
[30] Mohamed N, El-Masry HM. Aloe Vera gel extract and sunlight mediated synthesis of silver nanoparticles with highly effective antibacterial and anticancer activity. J Nanoanal. 2020;7(1):73–82.
[31] Tippayawat P, Phromviyo N, Boueroy P, Chompoosor A. Green synthesis of silver nanoparticles in aloe vera plant extract prepared by a hydrothermal method and their synergistic antibacterial activity. Peer J. 2016;4:e2589.
[32] Khan Y, Numan M, Ali M, Khali AT, Ali T, Abbas N, et al. Biosynthesized silver nanoparticles using different plant extracts as anti-cancer agent. J Nanomed Biother Discovery. 2017;7(154):2.
[33] Panda MK, Dhal NK, Kumar M, Mishra PM, Behera RK. Green synthesis of silver nanoparticles and its potential effect on phytopathogens. Mater Today Proc. 2021;35:233–8.
[34] Panda MK, Singh YD, Behera RK, Dhal NK. Biosynthesis of nanoparticles and their potential application in food and agricultural sector. Green nanoparticles. Cham: Springer; 2020. p. 213–25.
[35] Alwahibi MS, Soliman DA, Alonaizan A, Marraiki NA, El-Zaidy M, Al Subeie MS. Green biosynthesis of silver nanoparticle using Commiphora myrrh extract and evaluation of their antimicrobial activity and colon cancer cells viability. J King Saud Univ Sci. 2020;32(8):3372–9.
[36] Azizian-Shermeh O, Valizadeh M, Taherizadeh M, Beigomi M. Phytochemical investigation and phytosynthesis of eco-friendly stable bioactive gold and silver nan oparticles using petal extract of saffron (*Crocus sativus* L.) and study of their antimicrobial activities. Appl Nanosci. 2019;10:1–4.
[37] Arshad H, Muhammad AS, Saima S, Umer H. Salvadora persica mediated synthesis of silver nanoparticles and their antimicrobial efficacy. Sci Rep. 2021;11(1):1–11.
[38] Qais FA, Khan Mohd SA, Ahmed I, Althubiani AS. Potential of nanoparticles in combating *Candida infections*. Lett Drug Des Discov. 2019;16(5):478–91.
[39] Ghojavand S, Madani M, Karimi J. Green synthesis, characterization and antifungal activity of silver nanoparticles using stems and flowers of felty germander. J Inorg Organomet Polym Mater. 2020;30(8):2987–97.
[40] Paul A, Roychoudhury A. Go green to protect plants: repurposing the antimicrobial activity of biosynthesized silver nanoparticles to combat phytopathogens. Nanotechnol Environ Eng. 2021;6(1):1–22.